Environmental Science & Technology Letters

Letter

Exceptional Perrhenate/Pertechnetate Uptake and Subsequent Immobilization by a Low-Dimensional Cationic Coordination Polymer: Overcoming the Hofmeister Bias Selectivity

Lin Zhu, chengliang xiao, Xing Dai, Jie Li, Daxiang Gui, Daopeng Sheng, Lanhua Chen, Ruhong Zhou, Zhifang Chai, Thomas E. Albrecht-Schmitt, and Shuao Wang

Environ. Sci. Technol. Lett., **Just Accepted Manuscript** • Publication Date (Web): 31 May 2017

Exceptional Perrhenate/Pertechnetate Uptake and Subsequent Immobilization by a Low-Dimensional Cationic Coordination Polymer: Overcoming the Hofmeister Bias Selectivity

Lin Zhu[†, ‡, △], Chengliang Xiao[†, ‡, △], Xing Dai[†, ‡], Jie Li[†, ‡], Daxiang Gui[†, ‡], Daopeng Sheng[†, ‡], Lanhua Chen[†, ‡], Ruhong Zhou[†, ‡], Zhifang Chai[†, ‡], Thomas E. Albrecht-Schmitt[§], Shuao Wang[†, ‡, *]

[†] School for Radiological and Interdisciplinary Sciences (RAD-X), Soochow University, 215123, Suzhou, P. R. China

[‡] Collaborative Innovation Center of Radiation Medicine of Jiangsu Higher Education Institutions, 215123, Suzhou, P. R. China

[§] Department of Chemistry and Biochemistry, Florida State University, 95 Chieftain Way, Tallahassee, Florida 32306, United States

[△] These authors contribute equally

[*]Corresponding authors. Email: shuaowang@suda.edu.cn (SHUAO WANG); Tel: +86-512-65882573; Fax: +86-512-65883945.

ABSTRACT

We report one of the most efficient scavenger materials, a cationic crystalline coordination polymer SBN for trapping ReO_4^-, a surrogate for $^{99}TcO_4^-$ as an anionic radioactive contaminant of great concern. The uptake capacity for ReO_4^- reaches 786 mg/g, a value noticeably higher than the state of art anion-exchange resins and other inorganic or hybrid anion sorbents. Once being captured, ReO_4^- is greatly immobilized as almost no ReO_4^- can be eluted using large excess of nitrate, carbonate, and phosphate anions. The processes are featured by a complete and irreversible single-crystal-to-single-crystal structural transformation from SBN to the ReO_4^- incorporated phase (SBR). The coordination environments of NO_3^- and ReO_4^- probed by single crystal structures clearly unravel the underlying mechanism, where each ReO_4^- in SBR binds to multiple Ag^+ sites forming strong Ag−O−Re bonds, and to 4,4'-bipyridine through a dense hydrogen bond network. These structural insights lead to a significant difference of solubility product constants between SBN and SBR, which is further confirmed by first principle calculations showing a large binding energy difference of 35.61 kcal/mol. To the best of our knowledge, SBR is the least soluble perrhenate/pertechnetate salt reported, which may be considered as a potential waste form for direct immobilization of TcO_4^-.

INTRODUCTION

^{99}Tc is a long-lived fission product of ^{235}U or ^{239}Pu and primarily exists in aqueous solution as highly soluble, mobile, and stable TcO_4^- anion. Release of ^{99}Tc is a great concern in used fuel reprocessing, waste management, weapon testing, and nuclear accidents.[1,2] Technetium contamination has already been identified at several sites such as Hanford in southeastern Washington and Savannah River site in South Carolina.[3,4] Control of technetium release by waste form design and remediation of technetium pollution in the aqueous environment are therefore highly desirable, but are in fact of great challenge originating from the non-complexing nature of TcO_4^- anion.[5] Currently in Nuclear Waste Treatment and Immobilization, vitrification is the primary approach.[6] Because of the high temperature of vitrification, ^{99}Tc is volatilized and therefore only a portion is captured in the vitrified LAW waste form.[7] One proposed strategy is the chemical reduction from $Tc(VII)O_4^-$ to Tc(IV) and the separation from the aqueous solution is achieved by formation of insoluble Tc(IV) complexes.[8-11] These can be further incorporated into a pre-designed waste form containing crystallographically compatible sites for accommodating Tc(IV).[12-14] The most significant issue for this strategy is the re-oxidation of Tc(IV) back to Tc(VII) followed by the subsequent escaping from the host material.[14,15] Although many attempts have been focused on the kinetic retention of Tc(IV) in the lattice of waste form,[12,14,16] the re-oxidation seems to be inevitable during the long geological disposal period given this process is thermodynamically favorable under aerobic conditions.

This issue calls for the possibility of technetium disposal directly in the form of $Tc(VII)O_4^-$. Although this has been thought to be not applicable in light that almost all fifty known pertechnetate salts are sparingly soluble,[17] a recent study shows that pertechnetate can be incorporated into the lattice of sodalite as a potential waste form.[18-21] However, because of smaller ionic size of nitrate, nitrate anion possesses a clear preference to enter the sodalite cage. In addition, although a variety of anion-exchange materials have already been investigated for removing TcO_4^- from either nuclear waste stream or contaminated aqueous solutions including the state of

art anion-exchange polymeric organic resins,[22-24] molecular and supramolecular receptors,[25] layered double hydroxides (LDHs),[26,27] metal-organic frameworks (MOFs),[28,29] and porous organic materials,[30] they cannot be used for further immobilization of TcO_4^-, given these anion-exchange reactions are typically reversible.

Recently, Oliver et al[31] reported a low-dimensional cationic coordination polymer $[Ag(bipy)]NO_3$ (denoted as SBN, bipy= 4,4'-bipyridine) used as an effective adsorbent for the removal of ClO_4^- from aqueous solution with a very high capacity. In this work, we document our investigations of this type of material containing abundant coordination-available open Ag^+ site that can selectively bind to ReO_4^-/TcO_4^-, leading to capabilities of not only removing ReO_4^-/TcO_4^- from aqueous solution in a highly effective manner, but also greatly immobilizing ReO_4^-/TcO_4^- in its crystal lattice even in the presence of NO_3^- in large excess. ReO_4^- is used as a chemical surrogate for TcO_4^- in this study given their almost identical charge densities and many thermodynamic parameters except for the redox behaviors (**Table S1**).[32] The trapping mechanism was elucidated by a combination of single crystal X-ray diffraction analysis, thermodynamic analysis, and density function theory (DFT) analysis on binding. This work represents an in situ recrystallization route for TcO_4^- removal from aqueous by low-dimensional cationic MOFs and demonstrates the promising for this type of materials for technetium disposal.

■ MATERIALS AND METHODS

Synthesis and Characterization. SBN material was synthesized by hydrothermal method, as reported before (details were provided in the Supporting Information).[31,33] The detailed synthesis routes of other cationic materials for comparison, including NDTB-1,[34] Mg-Al-LDH,[35] and $Yb_3O(OH)_6Cl{\cdot}2H_2O$[36] were described in the Supporting Information. The commercial Purolite A532E anion-exchange resin was obtained from Purolite Co., Ltd. and dried at 60 ^oC for 24 h before use.

Batch Experiments. All the experiments were conducted at 25 ^oC using the batch

sorption method. The solid/liquid ratio performed in all batch experiments was 0.5 g/L. In a typical experiment, 10 mg of SBN was added into 20 mL of aqueous solution containing certain amounts of ReO_4^-. The resulting mixture was stirred for a desired contact time and separated with a 0.22 μm nylon membrane filter. The concentrations of ReO_4^- in aqueous solution were determined by Inductively Coupled Plasma Mass Spectrometry (ICP-MS, Thermo Scientific) and/or Inductively Coupled Plasma Optical Emission Spectrometry (ICP-OES, Thermo Fisher Scientific iCAP 7000). Single crystals of SBR were obtained directly from batch experiment when ReO_4^- was in small excess. After anion-exchange, the compounds were washed with deionized water several times, air-dried, and then characterized by Fourier Transform Infrared Spectroscopy (FT-IR) spectroscopy, Single-crystal X-ray Diffraction (SCXRD), Powder X-ray Diffraction (PXRD), and Scanning Transmission Electron Microscopy combined with an Energy Dispersive X-ray Spectrometer (STEM-EDS, Tecnai G2 spirit BioTwin).

SBN and SBR Dissolution Experiments. To determine the solubility product constant of the samples, the dissolution experiments were measured. Typically, 10 mg of sample (SBN or SBR) was added into 20 mL of aqueous solutions at various pHs. The concentrations of Ag^+ in aqueous solution were determined by ICP-MS. The thermodynamic parameters were calculated based on the solubility data. More details about the analyses are provided in the Supporting Information.

Computational Method. First-principle calculations based on density functional theory (DFT) were performed using Gaussian 09 program.[37] Two fragments of SBN and SBR extracted from the experimentally obtained crystal structures were chosen as the computational models. Geometry optimizations were performed at M062X-D3/SDD~6-31G(d, p) level, in which the M062X[38] functional combining with the D3 version of Grimme's dispersion[39] were employed, and the Stuttgart/Dresden relativistic effective core potentials (ECPs) with corresponding valence basis set (SDD)[40] and the standard Gaussian-type 6-31G(d, p) basis set[41] were applied for heavy atoms (Ag and Re) and light atoms (C, H, O and N), respectively.

The C, N, and Ag atoms of SBN and SBR frameworks were freeze during optimizations. Single-point energies were calculated for the complexes, the frameworks and anions after geometry optimizations at the same level and the binding energies (E_b) between anions and the frameworks were calculated by E_b = E(complex) – E(framework) – E(anion). The basis set superposition error (BSSE) has been excluded in calculating E_b.

RESULTS AND DISCUSSION

Synthesis and Characterization of SBN. The single-crystalline material of SBN crystals was synthesized by hydrothermal method.[31,33] Single-crystal X-ray Diffraction reveals the overall structure of SBN can be best described as a series of one-dimensional $[Ag(bipy)]^+$ (bipy= 4,4'-bipyridine) chains stacking together along *b* axis in a crossed manner (**Figures 1**, **S1a**, and **b**). Each Ag^+ ion is coordinated by two neutral 4,4'-bipyridine ligands while each 4,4'-bipyridine ligand bridges two Ag^+ ion within the chains with the Ag-N bonds of 2.163 Å. Weakly coordinated NO_3^- reside in the open space as the charge-balancing anion. The hydrolytic stability measurements was conducted before the sorption experiments, showing The SBN crystals are stable within pH range from 3 to 10 (**Figure S2**) while SBN crystals are completely dissolved below pH 2.

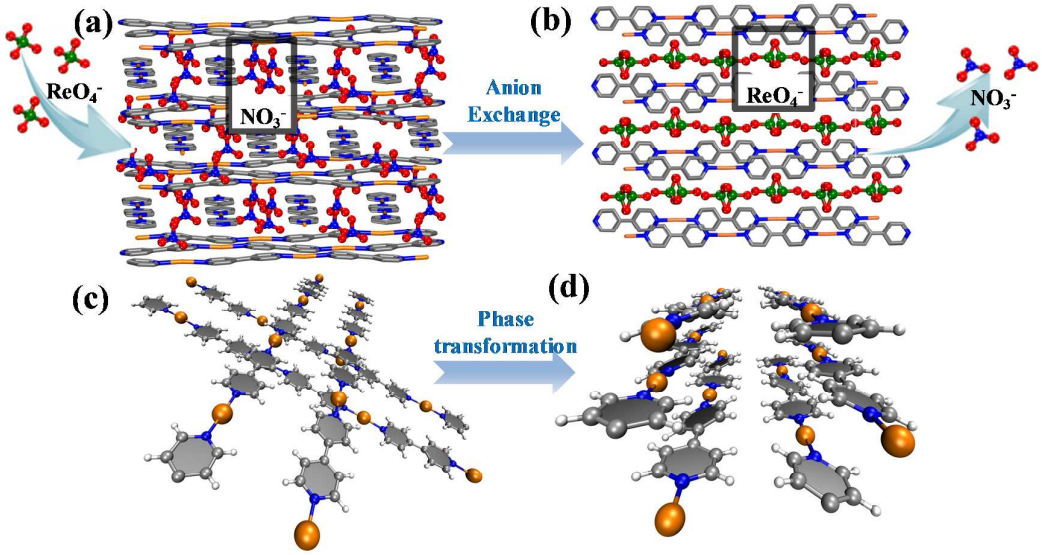

Figure 1. Crystal structures of SBN (a) and SBR (b) showing a single-crystal-to-single-crystal structural transformation mechanism; The black square regions represent locations of NO_3^- (a) and ReO_4^- (b); Packing modes of $[Ag(bipy)]^+$ chains of (c) SBN and (d) SBR in the 3D space.

ReO_4^- Sorption experiments. In order to check the anion-exchange properties of SBN towards TcO_4^-, the sorption experiments were investigated using the chemical surrogate ReO_4^-. Sorption kinetics of ReO_4^- on SBN was investigated as a function of contact time at pH 7 with an initial ReO_4^- concentration of 28 ppm and the solid/liquid ratio of 0.5 mg/ml. As shown in **Figure 2(a)**, the uptake kinetics of ReO_4^- by SBN is extremely fast as the sorption equilibrium can be reached within 10 minutes, where all ReO_4^- was completely removed from aqueous solution. The sorption rate is significantly faster than that of the commercial anion-exchange resin (A532E), specially designed for the removal of ClO_4^- and TcO_4^- under the identical condition, where the sorption equilibrium is reached after at least 2 h.[42] Compared with other reported MOFs with anion-exchange properties, SBN also possesses clear advantages. For example, the exchange equilibrium of ReO_4^- by UiO-66-NH_3^+ is reached after at least 24 h.[43] In practical application of TcO_4^- removal, the ultrafast removal kinetics would significantly decrease the contact time between the sorbents and radioactive waste solution, lowering the extent of material damage induced by radiation and hydrolysis.

The uptake isotherm experiments were conducted for 12 h and the results are shown in **Figure 2(b)**. Four other well-known anion sorbent materials, Mg-Al-LDH, NDTB-1, $Yb_3O(OH)_6Cl$, and Purolite A532E were also synthesized to evaluate their sorption properties towards ReO_4^- for comparison. Impressively, the sorption capacity of ReO_4^- by SBN reaches 714 mg ReO_4^-/g sorbent obtained from the fitting results based on the Langmuir model (**Figure S3 and Table S2**). This value is noticeably higher than most of the reported sorbents to date (**Table S3**) including all inorganic cationic materials and organic polymeric based ion exchange resins. When SBN was soaked in a solution with small molar excess of ReO_4^-, the sorption capacity was measured to be 786 mg/g and is close enough to the theoretic value of 767 mg/g,

suggesting all NO_3^- in the original material can be fully exchanged. Comparing with few examples of other reported cationic MOFs tested for ReO_4^-/TcO_4^- removal, the sorption capacity of SBN is also higher than that of UiO-66-NH_3^+ (159 mg/g),[43] SLUG-21 (602 mg/g),[28] and our recently reported SCU-100 (541 mg/g).[44]

We investigated the effect of pH ranging from 2 to 9 on the ReO_4^- sorption onto SBN. As shown in **Figure 2(c)**, the removal capacity increased from pH 2 to 5 and remained almost unchanged afterwards. Although SBN material fully dissolves at pH 2, the removal capacity is still quite high at ca. 200 mg/g, initially indicating that the recrystallization based phase transformation mechanism plays a role. The effect of competing NO_3^- amount on the ReO_4^- uptake was also studied given large quantities of NO_3^- is present in the real waste solution or natural water. For example, the molar ratio of NO_3^- / TcO_4^- is close to 300 in Hanford low-level waste melter off-gas scrubber stream.[26] As shown in **Figure 2(d)**, increasing the amounts of NO_3^- did not result in an obvious decrease of ReO_4^- removal percentage. Even in presence of 100-fold NO_3^-, the removal percentage was still as high as 90%, suggesting an excellent exchange selectivity towards ReO_4^- over NO_3^- possessed by SBN, which represents the opposite case of the incorporation of ReO_4^-/NO_3^- into sodalite.[18] Furthermore, the removal selectivity between ReO_4^-, CO_3^{2-}, $H_2PO_4^-$, SO_4^{2-}, Cl^- and ClO_4^- was also investigated and the results illustrate that SBN can completely remove ReO_4^- in the presence of other anions (**Figure S4**).

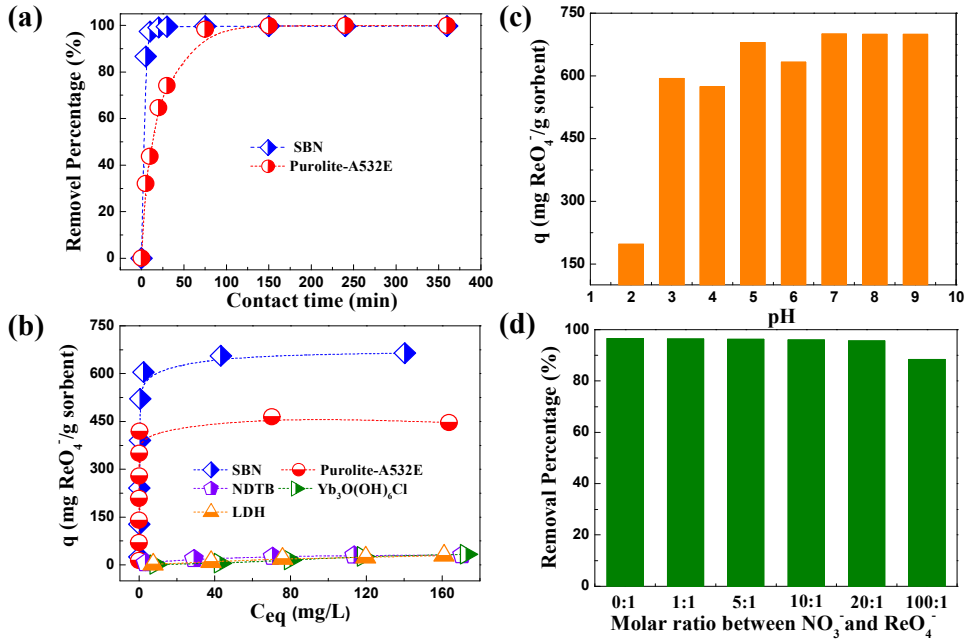

Figure 2. (a) Sorption kinetics data of ReO_4 into SBN and A532E; (b) Sorption isotherms of ReO_4^- by SBN compared with LDH, NDTB-1, Purolite-A532E, and $Yb_3O(OH)_6Cl$ materials; (c) Effect of pH on the sorption of ReO_4^- into SBN, (d) Effect of competing NO_3^- on the uptake of ReO_4^- by SBN.

Mechanisms and Thermodynamic study. Optical microscope photograph and SEM imaging show that gray block crystals of SBN disintegrates into smaller colorless needle crystals of SBR (**Figures S5 and S6**), indicating a complete phase transition occurs after the anion-exchange when ReO_4^- is in small excess. This is further confirmed by the PXRD measurements (**Figure S7b** and **S8**) and STEM-EDS mapping profiles (**Figure S9**) on the samples before and after the anion-exchange. In FT-IR spectra (**Figure S7a**), the arise of new peaks at 896 cm^{-1} and 860 cm^{-1} as well as the decrease of the peak at 1326 cm^{-1} is consistent with the complete substitution of NO_3^- by ReO_4^- in the solid.

More importantly, the crystal structure of needle phase SBR can be still clearly resolved by single-crystal X-ray diffraction (**Table S4**) and significantly deviates from that of SBN. This is surprising given the single-crystallinity of ion-exchange material is often ruined during the ion-exchange process. The mechanism of single-crystal

(SBN) to single-crystal (SBR) phase transformation is well described in **Figure 1**. although the major framework can be still best described by packing of one-dimensional $[Ag(bipy)]^+$ chains in 3D space, the packing mode undergoes a transition from the crossed packing in SBN (**Figures 1c, S1a** and **S1b**) to the parallel packing in SBR (**Figures 1d, S1c** and **S1d**). By a close examination on the coordination environments of NO_3^- in SBN and ReO_4^- in SBR, we propose that this dramatic change on the overall framework structure is indeed induced by change of charge-balancing anions and in fact occurs to better match the coordination requirement of ReO_4^-. In the structure of SBN (**Figure 3b** and **Table S5**), the three oxygen atoms within each NO_3^- binds to two Ag^+ cations with the Ag-O bonds ranging from 2.63 to 2.88 Å, and eight H atoms from 4,4'-bipyridine group forming a hydrogen bond network (O-H distances are from 2.21 to 3.93 Å). In comparison, the four oxygen atoms of each ReO_4^- in the structure of SBR (**Figure 3d**) is coordinated by obviously increased amounts (three) of Ag^+ at distances from 2.87 to 3.01 Å and a much denser hydrogen bond network containing 16 H atoms around each ReO_4^- at distances from 2.31 to 3.85 Å. This would result in a deep energy well for the effective stabilization of the ReO_4^- in the structure.

To quantitatively interpret the energetic difference between the coordination of NO_3^- and ReO_4^- in these two structures, we performed DFT calculations on the binding energy based on an optimized crystal structure model.[37-41] As more H and Ag^+ provide greater attractions for the central anions, the calculated binding energy between the anion and the cationic framework in SBR (-205.20 kcal/mol) becomes significantly larger in comparison to that in SBN (-169.59 kcal/mol). This large energetic difference of 35.61 kcal/mol is the intrinsic driving force accounting for large exchange capacity, rapid removal kinetics, and excellent sorption selectivity towards ReO_4^-. Furthermore, in order to qualitatively distinguish and assess the binding contributions from hydrogen bonds and O•••Ag^+ bonds respectively, we also calculated the O•••H binding energies between the central anions (NO_3^- and ReO_4^-) and the neutral frameworks (without Ag^+) by simply removing the Ag^+ cations in both

SBN and SBR fragments (for **Figure 3a** and **3c** models). Although the hydrogen bond network in SBR becomes much denser than that in SBN, the calculation results show a smaller O•••H binding energy difference (-24.39 kcal/mol in SBR and -30.10 kcal/mol in SBN). These relatively smaller O•••H binding energies (according to the total binding energies) imply that the major binding contributions are from O•••Ag^+ interactions, further highlighting the critical role of open Ag^+ sites in the selective removal of ReO_4^-/TcO_4^-.

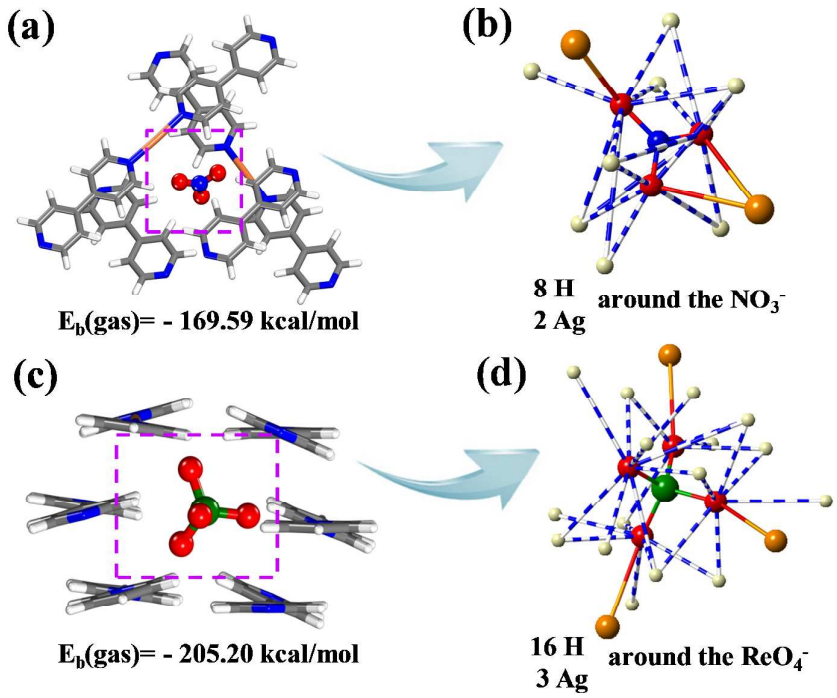

Figure 3. Fragment crystal structures of SBN (a) and SBR (c); A view of O•••H bond and O•••Ag^+ bond networks in SBN (b) and SBR (d); Atom colors: Ag = orange, N = blue, C = grey, H = white, Re = green, O = red, O•••H bond = blue/white bar, O•••Ag^+ bond = orange/red bar.

We propose the large energetic difference could further give rise to clear deviation on the thermodynamic behavior between SBN and SBR materials, especially the solubility in aqueous solution, which can be utilized for the elucidation of the selective anion-exchange process described by the **Equation (1)**.[45] Where L denotes the ligand (4,4'-bipyridine), K_1 and K_2 represent the thermodynamic equilibrium constant.

$$[\mathrm{Ag(bipy)}]\mathrm{NO}_{3(\mathrm{solid})} + \mathrm{ReO}_4^- + \mathrm{nH_2O} \overset{K1}{\leftrightarrow} [\mathrm{Ag}(H_2\mathrm{O})_\mathrm{n}]^+ + \mathrm{bipy} + \mathrm{NO}_3^- + \mathrm{ReO}_4^- \overset{K2}{\leftrightarrow} \mathrm{Ag(bipy)ReO}_{4(\mathrm{solid})} + \mathrm{NO}_3^- + \mathrm{nH_2O} \quad (1)$$

The corresponding experimental standard thermodynamic equilibrium constant (K^{θ}), reaction quotient (Q) and Gibbs free energy (ΔG(T)) values are present in **Table S6** and **Figure S10**. The thermodynamic driving force for ReO_4^- removal is attributed to the much lower solubility product constant of SBR compared to that of SBN. For the majority of pH conditions investigated (**Figures S10** and **S11**), the SBR is less soluble by at least three orders of magnitude, resulting in a spontaneous recrystallization based phase transformation process. Furthermore as shown in **Table S7**, the solubility product of SBR is as small as 2.16×10^{-13}, the smallest value among all known perrhenate and pertechnetate salts up to date.

Based on the large thermodynamic gap, the anion-exchange reaction appeared to be irreversible. Impressively as shown in **Figure S12,** the structure of SBR remained identical even after immersed into a concentrated (1 M) $NaNO_3$ solutions for 24 h while almost no noticeable amount of ReO_4^- leaks back to the aqueous solution. With the help of heating to 60 ^{o}C, SBR was not able to turn back to SBN, suggesting SBR is extremely robust in aqueous solution even containing huge excess of NO_3^-. We also checked the stability of SBR materials in the presence of excess of $H_2PO_4^-$ and CO_3^{2-} to be excellent as demonstrated by the dissolution studies and PXRD analysis on the solid sample after the dissolution studies (**Figure S13 and Table S8**). In addition, SBR is thermally stable up to 380 ^{o}C (**Figure S14**), which is again significant for technetium waste form design.

Environmental Implications. Searching for functional materials to efficiently remove TcO_4^- and host lattices to trap technetium as waste forms are both highly desirable and remains a significant challenge. Although different types of precipitation agent have been used for separating and trapping ^{99}Tc, there is significant opportunity for designing improved strategies and describing the

underlying molecular scale mechanisms that govern ^{99}Tc separation.[46-48] More importantly, previous investigation on the inorganic host lattice such as sodalite show incorporation preference towards NO_3^- over ReO_4^-/TcO_4^-. This phenomenon is typical following the well-known "Hofmeister bias"[49] because NO_3^- possesses higher charge density and smaller size than ReO_4^-/TcO_4^- and therefore higher affinity with the inorganic host lattice. What we show here is a low-dimensional coordination polymer materials equipped with abundant of open Ag^+ sites that are able to reverse the "Hofmeister bias" and shows an excellent anion-exchange selectivity towards ReO_4^-/TcO_4^- over NO_3^-. This material is capable of both removing and immobilizing TcO_4^- through a thermodynamically favorable phase transformation process, whose molecular mechanism is clearly elucidated by single crystal structures before and after uptake of the surrogate ReO_4^-, DFT calculation analysis on bonding, and solubility tests. We believe this study may provide a new viewpoint on how to deal with ^{99}Tc and SBR material should be further considered and evaluated for long-term storage of technetium without the concern of the redox activity.

■ ASSOCIATED CONTENT

Supporting Information

Details of materials and methods, additional data for SBN and SBR, are including nine figures and six tables. The Supporting Information is available free of charge via the Internet at http://pubs.acs.org.

■ AUTHOR INFORMATION

Corresponding Author

* E-mail: shuaowang@suda.edu.cn

■ ACKNOWLEDGMENTS

This work was supported by grants from the National Natural Science Foundation of China (21422704, U1532259, 11605118), the Science Foundation of Jiangsu Province (BK20140007, BK20150313), the State Key Laboratory of Pollution Control and Resource Reuse Foundation (PCRRF16003), a Project Funded by the Priority

Academic Program Development of Jiangsu Higher Education Institutions (PAPD) and Jiangsu Provincial Key Laboratory of Radiation Medicine and Protection, "Young Thousand Talented Program" in China. TEA-S is supported by the U.S. Department of Energy, Office of Science, Office of Basic Energy Sciences, Heavy Elements Chemistry Program, under Award Number DE-FG02-13ER16414.

REFERENCES

(1) Natal'ya, N. P.; Ivan, G. T.; Sergei, I. R.; Boris, F. M. Technetium: behaviour during reprocessing of spent nuclear fuel and in environmental objects. *Russ. Chem. Rev.* **2003**, *72*, 101-121.

(2) Standring, W. J. F.; Oughton, D. H.; Salbu, B. Potential remobilization of Cs-137, Co-60, Tc-99 and Sr-90 from contaminated Mayak sediments river and estuary environments. *Environ. Sci. Technol.* **2002**, *36*, 2330-2337.

(3) Banerjee, D.; Kim, D.; Schweiger, M. J.; Kruger, A. A.; Thallapally, P. K. Removal of TcO_4^- ions from solution: materials and future outlook. *Chem. Soc. Rev.* **2016**, *45*, 2724-2739.

(4) Lukens, W. W.; Shuh, D. K.; Schroeder, N. C.; Ashley, K. R. Identification of the non-pertechnetate species in Hanford waste tanks, Tc(I)-carbonyl complexes. *Environ. Sci. Technol.* **2004**, *38*, 229-233.

(5) Steinhauser, G. Fukushima's Forgotten Radionuclides: A Review of the Understudied Radioactive Emissions. *Environ. Sci. Technol.* **2014**, *48*, 4649-4663.

(6) Gin, S.; Abdelouas, A.; Criscenti, L. J.; Ebert, W. L.; Ferrand, K.; Geisler, T.; Harrison, M. T.; Inagaki, Y.; Mitsui, S.; Mueller, K. T.; Marra, J. C.; Pantano, C. G.; Pierce, E. M.; Ryan, J. V.; Schofield, J. M.; Steefel, C. I.; Vienna, J. D. An international initiative on long-term behavior of high-level nuclear waste glass. *Mater. Today* **2013**, *16*, 243-248.

(7) Childs, B. C.; Poineau, F.; Czerwinski, K. R.; Sattelberger, A. P. The nature of the volatile technetium species formed during vitrification of borosilicate glass. *J. Radioanal. Nucl. Chem.* **2015**, *306*, 417-421.

(8) Pierce, E. M.; Lukens, W. W.; Fitts, J. P.; Jantzen, C. M.; Tang, G. Experimental determination of the speciation, partitioning, and release of perrhenate as a chemical surrogate for pertechnetate from a sodalite-bearing multiphase ceramic waste form. *Appl. Geochem.* **2014**, *42*, 47-59.

(9) Yang, J.; Kukkadapu, R. K.; Dong, H.; Shelobolina, E. S.; Zhang, J.; Kim, J. Effects of redox cycling of iron in nontronite on reduction of technetium. *Chem. Geol.* **2012**, *291*, 206-216.

(10) Eagling, J.; Worsfold, P. J.; Blake, W. H.; Keith-Roach, M. J. Mobilization of Technetium from Reduced Sediments under Seawater Inundation and Intrusion Scenarios. *Environ. Sci. Technol.* **2012**, *46*, 11798-11803.

(11) Icenhower, J. P.; Qafoku, N. P.; Zachara, J. M.; Martin, W. J. The biogeochemistry of technetium: a review of the behavior of an artificial element in the natural environment. *Am. J. Sci.* **2010**, *310*, 721-752.

(12) Lee, M.-S.; Um, W.; Wang, G.; Kruger, A. A.; Lukens, W. W.; Rousseau, R.; Glezakou, V.-A. Impeding Tc-99(IV) mobility in novel waste forms. *Nat. Commun.* **2016**, *7*.

(13) Burton-Pye, B. P.; Radivojevic, I.; McGregor, D.; Mbomekalle, I. M.; Lukens, W. W., Jr.; Francesconi, L. C. Photoreduction of Tc-99 Pertechnetate by Nanometer-Sized Metal Oxides: New Strategies for Formation and Sequestration of Low-Valent Technetium. *J. Am. Chem. Soc.* **2011**, *133*, 18802-18815.

(14) Um, W.; Chang, H.-S.; Icenhower, J. P.; Lukens, W. W.; Serne, R. J.; Qafoku, N. P.; Westsik, J. H., Jr.; Buck, E. C.; Smith, S. C. Immobilization of 99-Technetium (VII) by Fe(II)-Goethite and Limited Reoxidation. *Environ. Sci. Technol.* **2011**, *45*, 4904-4913.

(15) Burke, I. T.; Boothman, C.; Lloyd, J. R.; Livens, F. R.; Charnock, J. M.; McBeth, J. M.; Mortimer, R. J. G.; Morris, K. Reoxidation behavior of technetium, iron, and sulfur in estuarine sediments. *Environ. Sci. Technol.* **2006**, *40*, 3529-3535.

(16) Marshall, T. A.; Morris, K.; Law, G. T. W.; Mosselmans, J. F. W.; Bots, P.; Parry, S. A.; Shaw,

S. Incorporation and Retention of 99-Tc(IV) in Magnetite under High pH Conditions. *Environ. Sci. Technol.* **2014**, *48*, 11853-11862.

(17) Boitsova, T. A.; Babain, V. A.; Murzin, A. A.; Lumpov, A. A.; Krasnikov, L. V.; Kol'tsova, T. I. Precipitation of pertechnetate ion from nitric acid solutions using complexes of copper(II) with heterocyclic N-donor ligands. *J. Radioanal. Nucl. Chem.* **2016**, *307*, 1519-1527.

(18) Dickson, J. O.; Harsh, J. B.; Flury, M.; Lukens, W. W.; Pierce, E. M. Competitive Incorporation of Perrhenate and Nitrate into Sodalite. *Environ. Sci. Technol.* **2014**, *48*, 12851-12857.

(19) Pierce, E. M.; Lilova, K.; Missimer, D. M.; Lukens, W. W.; Wu, L.; Fitts, J.; Rawn, C.; Huq, A.; Leonard, D. N.; Eskelsen, J. R.; Woodfield, B. F.; Jantzen, C. M.; Navrotsky, A. Structure and Thermochemistry of Perrhenate Sodalite and Mixed Guest Perrhenate/Pertechnetate Sodalite. *Environ. Sci. Technol.* **2017**, *51*, 997-1006.

(20) Dickson, J. O.; Harsh, J. B.; Flury, M.; Pierce, E. M. Immobilization and exchange of perrhenate in sodalite and cancrinite. *Micropor. Mesopor. Mat.* **2015**, *214*, 115-120.

(21) Dickson, J. O.; Harsh, J. B.; Lukens, W. W.; Pierce, E. M. Perrhenate incorporation into binary mixed sodalites: The role of anion size and implications for technetium-99 sequestration. *Chem. Geol.* **2015**, *395*, 138-143.

(22) Bonnesen, P. V.; Brown, G. M.; Alexandratos, S. D.; Bavoux, L. B.; Presley, D. J.; Patel, V.; Ober, R.; Moyer, B. A. Development of bifunctional anion-exchange resins with improved selectivity and sorptive kinetics for pertechnetate: Batch-equilibrium experiments. *Environ. Sci. Technol.* **2000**, *34*, 3761-3766.

(23) Burgeson, I. E.; Deschane, J. R.; Blanchard, D. L. Removal of technetium from Hanford tank waste supernates. *Separ. Sci. Technol.* **2005**, *40*, 201-223.

(24) Bond, A. H.; Gula, M. J.; Harvey, J. T.; Duffey, J. M.; Horwitz, E. P.; Griffin, S. T.; Rogers, R. D.; Collins, J. L. Flowsheet feasibility studies using ABEC resins for removal of pertechnetate from nuclear wastes. *Ind. Eng. Chem. Res.* **1999**, *38*, 1683-1689.

(25) Eble, B.; Berning, D.; Barnes, C. L.; Katti, K. V.; Jurisson, S. Phosphinimine complexes of technetium(VII): X-ray crystal structure of $[Ph_3P = NH_2^+][TcO_4^-]$. *J. Chem. Crystallogr.* **1999**, *29*, 39-43.

(26) Wang, S.; Yu, P.; Purse, B. A.; Orta, M. J.; Diwu, J.; Casey, W. H.; Phillips, B. L.; Alekseev, E. V.; Depmeier, W.; Hobbs, D. T.; Albrecht-Schmitt, T. E. Selectivity, Kinetics, and Efficiency of Reversible Anion Exchange with TcO_4^- in a Supertetrahedral Cationic Framework. *Adv. Funct. Mater.* **2012**, *22*, 2241-2250.

(27) Goh, K.-H.; Lim, T.-T.; Dong, Z. Application of layered double hydroxides for removal of oxyanions: A review. *Water Res.* **2008**, *42*, 1343-1368.

(28) Fei, H.; Bresler, M. R.; Oliver, S. R. J. A New Paradigm for Anion Trapping in High Capacity and Selectivity: Crystal-to-Crystal Transformation of Cationic Materials. *J. Am. Chem. Soc.* **2011**, *133*, 11110-11113.

(29) Bai, Z.; Wang, Y.; Li, Y.; Liu, W.; Chen, L.; Sheng, D.; Juan, D.; Chai, Z.; Albrecht-Schmitt, T. E.; Wang, S. First Cationic Uranyl-Organic Framework with Anion-Exchange Capabilities. *Inorg. Chem.* **2016**, *55*, 6358-6360.

(30) Banerjee, D.; Elsaidi, S. K.; Aguila, B.; Li, B.; Kim, D.; Schweiger, M. J.; Kruger, A. A.; Doonan, C. J.; Ma, S.; Thallapally, P. K. Removal of Pertechnetate-Related Oxyanions from Solution Using Functionalized Hierarchical Porous Frameworks. *Chem. Eur. J.* **2016**, *22*, 17581-17584.

(31) Colinas, I. R.; Silva, R. C.; Oliver, S. R. J. Reversible, Selective Trapping of Perchlorate

from Water in Record Capacity by a Cationic Metal-Organic Framework. *Environ. Sci. Technol.* **2016**, *50*, 1949-1954.

(32) Lukens, W. W.; McKeown, D. A.; Buechele, A. C.; Muller, I. S.; Shuh, D. K.; Pegg, I. L. Dissimilar behavior of technetium and rhenium in borosilicate waste glass as determined by X-ray absorption spectroscopy. *Chem. Mater.* **2007**, *19*, 559-566.

(33) Yaghi, O. M.; Li, H. L. T-shaped molecular building units in the porous structure of Ag(4,4'-bpy)·NO_3. *J. Am. Chem. Soc.* **1996**, *118*, 295-296.

(34) Wang, S.; Alekseev, E. V.; Diwu, J.; Casey, W. H.; Phillips, B. L.; Depmeier, W.; Albrecht-Schmitt, T. E. NDTB-1: a supertetrahedral cationic framework that removes TcO_4^- from solution. *Angew. Chem. Int. Ed.* **2010**, *49*, 1057-1060.

(35) Constantino, V. R. L.; Pinnavaia, T. J. Basic properties of $Mg_{1-x}(2+)Al_x(3+)$ layered double hydroxides intercalated by carbonate, hydroxide chloride and sulfate anions. *Inorg. Chem.* **1995**, *34*, 883-892.

(36) Goulding, H. V.; Hulse, S. E.; Clegg, W.; Harrington, R. W.; Playford, H. Y.; Walton, R. I.; Fogg, A. M. $Yb_3O(OH)_6Cl\cdot 2H_2O$: An Anion-Exchangeable Hydroxide with a Cationic Inorganic Framework Structure. *J. Am. Chem. Soc.* **2010**, *132*, 13618-13620.

(37) Frisch, M. J.; Trucks, G. W.; Schlegel, H. B.; Scuseria, G. E.; Robb, M. A.; Cheeseman, J. R.; Scalmani, G.; Barone, V.; Mennucci, B.; Petersson, G. A.; Nakatsuji, H.; Caricato, M.; Li, X.; Hratchian, H. P.; Izmaylov, A. F.; Bloino, J.; Zheng, G.; Sonnenberg, J. L.; Hada, M.; Ehara, M.; Toyota, K.; Fukuda, R.; Hasegawa, J.; Ishida, M.; Nakajima, T.; Honda, Y.; Kitao, O.; Nakai, H.; Vreven, T.; J. A. Montgomery, J.; Peralta, J. E.; Ogliaro, F.; Bearpark, M.; Heyd, J. J.; Brothers, E.; Kudin, K. N.; Staroverov, V. N.; Keith, T.; Kobayashi, R.; Normand, J.; Raghavachari, K.; Rendell, A.; Burant, J. C.; Iyengar, S. S.; Tomasi, J.; Cossi, M.; Rega, N.; Millam, J. M.; Klene, M.; Knox, J. E.; Cross, J. B.; Bakken, V.; Adamo, C.; Jaramillo, J.; Gomperts, R.; Stratmann, R. E.; Yazyev, O.; Austin, A. J.; Cammi, R.; Pomelli, C.; Ochterski, J. W.; Martin, R. L.; Morokuma, K.; Zakrzewski, V. G.; Voth, G. A.; Salvador, P.; Dannenberg, J. J.; Dapprich, S.; Daniels, A. D.; Farkas, O.; Foresman, J. B.; Ortiz, J. V.; Cioslowski, J.; Fox, D. J.: Gaussian 09, Revision E.01. 2013.

(38) Zhao, Y.; Truhlar, D. G. The M06 suite of density functionals for main group thermochemistry, thermochemical kinetics, noncovalent interactions, excited states, and transition elements: two new functionals and systematic testing of four M06-class functionals and 12 other functionals. *Theor. Chem. Acc.* **2008**, *120*, 215-241.

(39) Grimme, S.; Antony, J.; Ehrlich, S.; Krieg, H. A consistent and accurate ab initio parametrization of density functional dispersion correction (DFT-D) for the 94 elements H-Pu. *J. Chem. Phys.* **2010**, *132*.

(40) Andrae, D.; Häußermann, U.; Dolg, M.; Stoll, H.; Preuß, H. Energy-adjustedab initio pseudopotentials for the second and third row transition elements. *Theor. Chim. Acta.* **1990**, *77*, 123-141.

(41) Hehre, W. J.; Ditchfie.R; Pople, J. A. Self-Consistent Molecular-Orbital Methods .12. Further Extensions Of Gaussian-Type Basis Sets for Use In Molecular-Orbital Studies Of Organic-Molecules. *J. Chem. Phys.* **1972**, *56*, 2257-2261.

(42) Zhu, Y.; Gao, N.; Wang, Q.; Wei, X. Adsorption of perchlorate from aqueous solutions by anion exchange resins: Effects of resin properties and solution chemistry. *Colloid Surface. A* **2015**, *468*, 114-121.

(43) Banerjee, D.; Xu, W.; Nie, Z.; Johnson, L. E. V.; Coghlan, C.; Sushko, M. L.; Kim, D.;

Schweiger, M. J.; Kruger, A. A.; Doonan, C. J.; Thallapally, P. K. Zirconium-Based Metal-Organic Framework for Removal of Perrhenate from Water. *Inorg. Chem.* **2016**, *55*, 8241-8243.

(44) Sheng, D.; Zhu, L.; Xu, C.; Xiao, C.; Wang, Y.; Wang, Y.; Chen, L.; Diwu, J.; Chen, J.; Chai, Z.; Albrecht-Schmitt, T. E.; Wang, S. Efficient and Selective Uptake of TcO_4^- by a Cationic Metal-Organic Framework Material with Open Ag^+ Sites. *Environ. Sci. Technol.* **2017**, *51*, 3471-3479.

(45) Cui, X.; Khlobystov, A. N.; Chen, X.; Marsh, D. H.; Blake, A. J.; Lewis, W.; Champness, N. R.; Roberts, C. J.; Schroder, M. Dynamic Equilibria in Solvent-Mediated Anion, Cation and Ligand Exchange in Transition-Metal Coordination Polymers: Solid-State Transfer or Recrystallisation? *Chem. Eur. J.* **2009**, *15*, 8861-8873.

(46) Mausolf, E.; Droessler, J.; Poineau, F.; Hartmann, T.; Czerwinski, K. Tetraphenylpyridinium pertechnetate: a promising salt for the immobilization of technetium. *Radiochim. Acta* **2012**, *100*, 325-328.

(47) Chadwick, T. C. 1, 2, 4, 6-Tetraphenylpyridinium acetate as a new anion precipitant. *Anal. Chem.* **1976**, *48*, 1201-1202.

(48) German, K. E.; Grigoriev, M. S.; Den Auwer, C.; Maruk, A. Y.; Obruchnikova, Y. A. Structure and solubility of tetrapropylammonium pertechnetate and perrhenate. *Russ. J. Inorg. Chem.* **2013**, *58*, 691-694.

(49) Custelcean, R.; Moyer, B. A. Anion separation with metal-organic frameworks. *Eur. J. Inorg. Chem.* **2007**, 1321-1340.

For Table of Contents Use Only

Exceptional Perrhenate/Pertechnetate Uptake and Subsequent Immobilization by a Low-Dimensional Cationic Coordination Polymer: Overcoming the Hofmeister Bias Selectivity

Lin Zhu[†, ‡, △], Chengliang Xiao[†, ‡, △], Xing Dai[†, ‡], Jie Li[†, ‡], Daxiang Gui[†, ‡], Daopeng Sheng[†, ‡], Lanhua Chen[†, ‡], Ruhong Zhou[†, ‡], Zhifang Chai[†, ‡], Thomas E. Albrecht-Schmitt[§], Shuao Wang[†, ‡]